Relationship between Mesophase and Semicrystalline Morphology in Smectic Liquid Crystalline Polymers

S. D. Hudson*,† and A. J. Lovinger

AT&T Bell Laboratories, Murray Hill, New Jersey 07974

M. A. Gomez, J. Lorente, C. Marco, and J. G. Fatou

Instituto de Ciencia y Tecnologia de Polimeros, Juan de la Cierva 3, 28006 Madrid, Spain

Received December 9, 1993; Revised Manuscript Received March 3, 1994®

ABSTRACT: The semicrystalline morphology of a semiflexible smectic polyester is investigated by high-resolution electron microscopy. Images combining diffraction and phase contrast allow simultaneous visualization of the mesomorphic and semicrystalline phases. A smectic C_2 mesophase is confirmed by electron diffraction of quenched (noncrystalline) specimens. A new disordered–uniaxial model is developed to evaluate the molecular tilt in smectic mesophases in which the *layers* rather than the molecules are aligned. Biaxial symmetry for small selected areas (<200 nm) and uniaxial symmetry, about the layer normal, for larger areas requires extended polymer chains to be twisted and entangled around one another. These molecular entanglements, unique to *polymeric* smectic mesophases, are argued to limit crystal growth to very thin lamellae (8 nm) and low crystallinity (~40%). In spite of the small thickness of the crystals, the coherence length normal to the lamellae is large.

Introduction

Liquid crystalline and semicrystalline order in polymers gives rise to many useful optical, rheological, and mechanical properties.[1] Polymers exhibit a variety of phases, and many of the newer high-performance polymers have nematic or smectic, as well as semicrystalline, phases.[2] It is important to understand how molecular organization in one phase influences transformation to another; often the polymeric nature of the molecules plays a critical role that is not operative in low-molecular-weight materials. In this study, we examine morphologically the smectic-to-semicrystalline phase transition in polymers.

Previously, the nematic-to-crystal transformation of liquid crystal polymers (LCP's) has been investigated. In the nematic mesophase, molecules are orientationally ordered, yet lack long-range positional order. Positional order develops as the material crystallizes (in a lamellar morphology).[3,4] If the crystal–nucleation density is high, little reorientation occurs upon crystallization and the resultant morphology allows visualization of disclination defects. This crystallization technique has been exploited to study material properties[5,6] and disclination interactions.[7] The kinetics of crystallization from various mesophases have also been studied, showing that the "preconditioning" temperature in the nematic mesophase has a strong influence.[8] The chain conformation is presumably a function of temperature. In the semicrystalline phase, molecular folds are implied by the small thickness and higher density of the lamellar crystallites.[9] It is not known whether a corresponding number of these folds (hairpins) is present also in the nematic state.[10]

In smectic mesophases, one-dimensional positional order exists as well as orientational order. Previous microscopy has probed the structure of smectic mesophases and their associated defects.[11,12] One might suppose that crystallization would be facilitated by smectic order. However, a recent NMR investigation indirectly suggests that entanglements may be present in the smectic mesophase. These might inhibit crystallization, and, conversely, crystallization may disrupt smectic order.[13] Through morphological investigation, we address this question here and evaluate the molecular order in both smectic and semicrystalline phases.

Method

In order to probe smectic order, we selected a thermotropic polymer with an easily identified and broad smectic phase:[14]

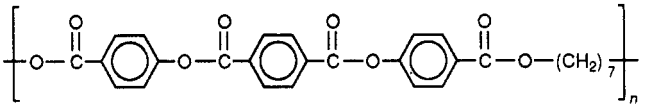

The glass transition temperature of this main-chain liquid crystalline polymer is ~65 °C. Semicrystalline material melts at 175 °C to a smectic mesophase, which is quite stable and does not melt to the isotropic phase until 295 °C. The structure of this material has been investigated previously by X-ray diffraction and vibrational spectroscopy.[15] In the liquid crystalline phase, a low-angle reflection characteristic of a smectic mesophase was observed, and a layer spacing of 23.3 Å was measured. By assuming an all-trans conformation in the methylene spacer, a structure was proposed which accommodated the mesogens in a smectic C_2 arrangement with a layer spacing of 24 Å. Further evidence[16] and results from infrared studies of poly[decamethyleneterephthaloyl bis(4-oxybenozate)][17] do not rule out the possibility of a GTG′ conformation in the methylene spacer.

Thin films for electron microscopic investigation were prepared as follows. A few milligrams of the polymer were sheared onto a glass slide heated to 225 °C in a N_2 atmosphere. The LCP was quenched to room temperature by rapidly removing the slide from the heat and plunging it into water. Polarized-light microscopy verified high orientation in the thin polymer film. The polymer was removed from the glass slide by first overcasting a thick layer of poly(acrylic acid) (PAA) from concentrated aqueous solution. After thorough drying in vacuum, the PAA became glassy and was detached, carrying with it an ultrathin film of LCP, suitable for TEM. Evaporation of amorphous carbon provided mechanical integrity to the LCP film, which was retrieved by dissolving the PAA and mounting it onto an EM grid.

The thin LCP film (50–100 nm in thickness) was then treated in one of three ways before TEM examination. First "quenched" samples were prepared by heating to 200 °C in a N_2 atmosphere for 3 min and then rapidly quenching to ambient temperature

† Present address: Department of Macromolecular Science, Case Western Reserve University, Cleveland, OH 44106.

• Abstract published in *Advance ACS Abstracts*, April 15, 1994.

0024-9297/94/2227-3357$04.50/0

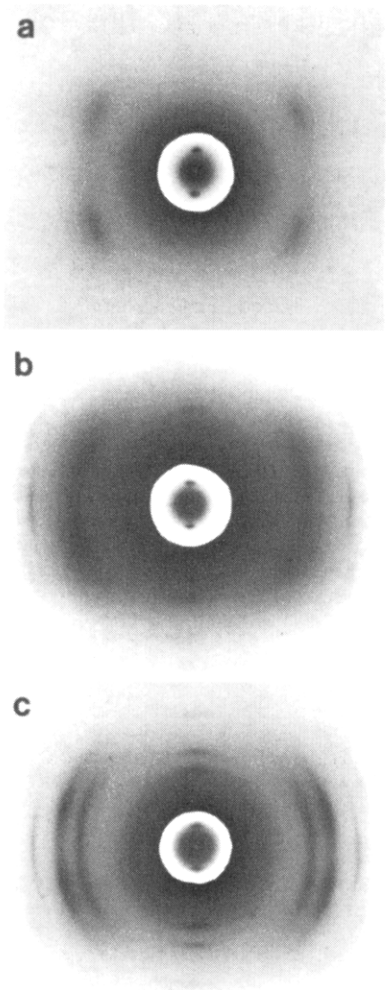

Figure 1. Electron diffraction of (a) quenched, (b) annealed, and (c) solvent-treated LCP films. The equatorial direction is horizontal, and the meridional or averaged chain axis is vertical. Weaker exposure is used to show the 001 reflection.

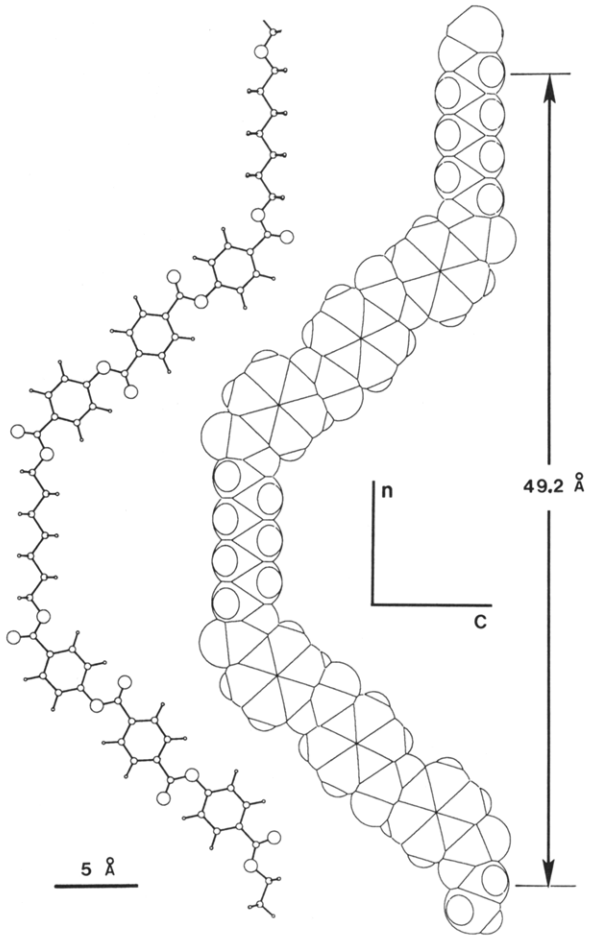

Figure 2. Extended chain conformation, viewed face-on, using the following bond distances (Å): C–C, 1.53; C–O, 1.42; OC–O, 1.33; C=O, 1.20; C=C, 1.39; ArC–O, 1.46; ArC–C, 1.50. Bond angles (deg): C–O–Ar, 119.0; Ar–C–O, 110.0; C–O–C, 116.5; C–C–C, 112.7. The bilayer repeat is 49.2 Å, and the **n**- and **C**-directors are marked. **n** is the smectic layer normal, and **C** is the *projection* of the mesogen axis onto the layer plane.

in air. An "annealed" sample was prepared by first heating, as before, to 200 °C and then quenching in a similar N_2 chamber at 140 °C; after 34 min, this sample was further quenched to room temperature. Finally, another sample was "solvent treated": this sample was first quenched from 200 °C to ambient, as before, and then exposed to methanol at 40 °C for 3 h. Finally, films of each preparation were examined at 200 kV using a JEOL 2000FX TEM. Electron diffraction obtained using a Philips 200-kV CM20 TEM operating in microdiffraction mode was used to evaluate the fine-scale texture of these films.

Results and Discussion

Electron diffraction of the quenched film (Figure 1a) confirms a tilted mesophase. At low angles, a sharp meridional reflection gives the layer spacing of 23.4 Å, in agreement with previous X-ray diffraction.[15] At wide angles, the scattering arising from lateral correlations is diffuse with maxima off-equatorial, at an azimuthal angle, β_{max}, measured from the equator, of approximately 28°. The molecular chains are thus inclined in some fashion to the layer normal, which is aligned. Molecular inclination is consistent with an extended model conformation, in which the mesogens tilt in alternate directions (Figure 2), forming a tilted bilayer smectic C_2 (S_{C_2}).[18] Alternatively, this type of smectic mesophase has been termed C_p[19] or unconventional.[20] The model bilayer repeat is 49.2 Å, but by symmetry, only the 002 reflection, and not the 001, would be observable by diffraction (Figure 1a), having a periodicity of 24.6 Å. Each "half"-layer contains a single monomer repeat, and the mesogens are each tilted 48° from the layer normal. The agreement of the layer spacing with experiment is very good considering such a long monomer, and the mesogen tilt is also reasonable, as we shall show.

Molecular organization can be assessed by the symmetry of the diffraction pattern and how it depends upon the selected-area diameter. When the diameter of the selected-area electron beam is at least 200 nm, the diffraction pattern (Figure 1a) is cylindrically symmetric about the smectic layer normal, as confirmed by tilting of the specimen about an axis parallel to the layer normal. Furthermore, the intensities of the wise-angle peaks are equal. Uniaxial symmetry at this scale, however, does not imply smectic A symmetry. By definition, any smectic C mesophase is biaxial, and the biaxial character of the smectic C_2 phase is confirmed by smaller-diameter selected-area diffraction. When the electron beam is less than 200 nm in diameter, β_{max} depends upon which area of the specimen is illuminated, as should be the case when the **C**-director varies with position (Figures 3 and 6). Since variation of the **C**-director is found upon translation parallel (as well as perpendicular) to **n**, the chains are twisted about their axes. (We define θ as the angle of molecular twist about **n**, i.e., the orientation of the C-director.) Because the face of the chain (Figure 3a) (19 or 20 Å) is much larger than its edge (Figure 3b) (~4.3 Å),

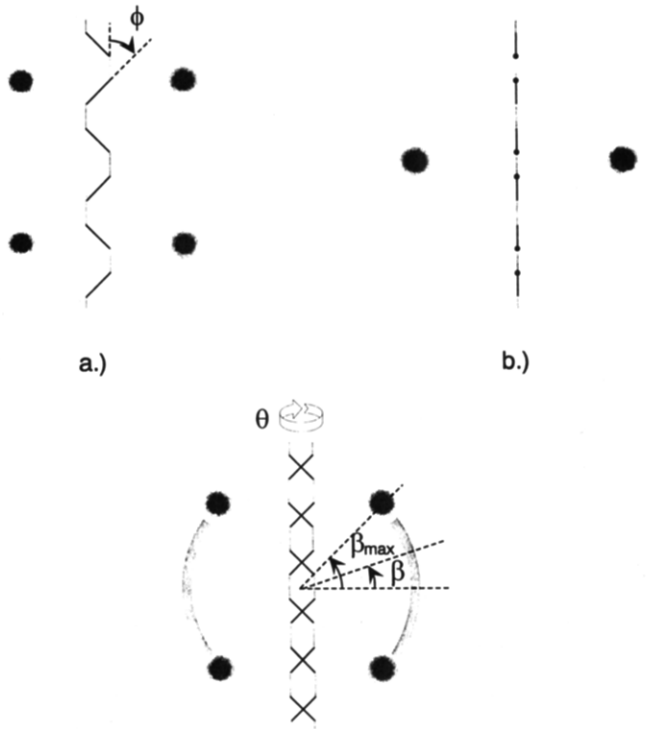

Figure 3. Schematic representation of wide-angle electron diffraction as a function of molecular rotation about the chain axis. The extended chain conformation (Figure 2) is pictured in the center of each diffraction pattern. The mesogen and spacer are represented by dark and light lines, respectively. (a) When the chain is face-on, i.e., the electron beam is perpendicular to **C** ($\theta = \pi/2$), a four-point wide-angle pattern is produced. If the chain is rotated about its axis, the azimuthal angle between the wide-angle peaks is reduced. (b) When the chain is edge-on, i.e., the electron beam is parallel to **C** ($\theta = 0$), the wide-angle peaks coalesce on the equator, forming a two-point pattern. The dots at mesogen ends indicate the end that is tilting toward the view direction. (c) If the sampling of chains is cylindrically symmetric (θ is uniformly distributed between 0 and $\pi/2$), wide-angle arcs are produced.

packing constraints require that twisting chains must also twist around one another (Figure 4a); i.e., they are *entangled*.[21]

Having established uniaxial symmetry of the diffraction pattern Figure 1a, we now address the mesogen tilt angle. Previously, it has been assumed that the azimuthal angle of largest intensity, β_{max}, is the angle, ϕ, at which the mesogens are inclined.[18,20,22,23] However, this assumption neglected the essential difference between ordinary smectic C and smectic C_2. Here we develop a simple model that reexamines the relationship between β_{max} and ϕ. For ordinary smectic C materials, in which the *molecules* may be oriented and the *layers tilted*, the angle that the *layer* diffraction peak makes with the meridian *is* the molecular tilt angle. In contrast, as a consequence of the alternating tilt of smectic C_2, it is impossible to uniformly align the mesogens. When the polymer chain is aligned, it is the smectic *layers*, and not the *mesogens*, which may be oriented. Since rodlike objects (mesogens) are tilted, rather than planes, there is wide-angle scattering at azimuthal angles intermediate to the maxima (Figure 3c). A key point of our model is that orientational disorder within the layers causes the peak in the diffraction arc to broaden and shift to a smaller azimuthal angle, β_{max}. Cylindrical symmetry and orientational disorder also apply to the drawn fibers investigated previously,[18,20,22,23] and

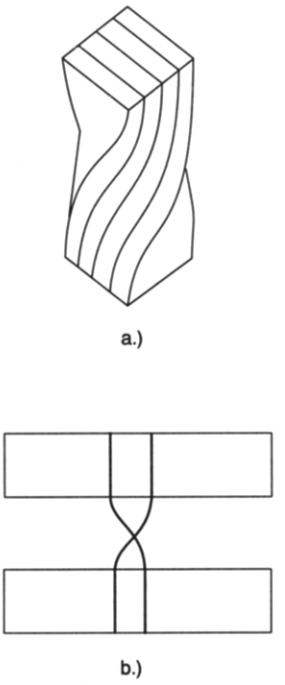

Figure 4. (a) Schematic of twisted, entangled chains of anisometric cross section. (b) Schematic of an entanglement between two crystals.

we expect similar differences between β_{max} and ϕ in these cases. Differences between the azimuthal angle of diffraction and the molecular tilt angle are not observed in ordinary smectic C's, because the Fourier transform of periodic parallel planes is a point, and cylindrical symmetry does not introduce diffraction at intermediate azimuthal angles. Furthermore, orientational disorder within ordinary smectic C layers does not shift the diffraction peak significantly—only causing the diffractionn peak to broaden.

The basic conclusions of our disordered uniaxial model are described in the previous paragraph, and now we describe its derivation. If the distribution of twist angles, θ, about the chain axis is uniform, then the distribution function of the scattered intensity expressed in terms of azimuth, β, from the equator is:

$$I(\beta) = (\sin^2\phi - \sin^2\beta)^{-0.5}, \quad \beta \le \phi$$

$$I(\beta) = 0, \quad \beta > \phi \tag{1}$$

which derives from the relation between θ and β, $\sin\beta = \sin\phi \sin\theta$ (see schematic Figure 3), and from the typical polarization factor, $\cos\beta$. For perfectly oriented layers, the intensity is thus sharply peaked at ϕ. When orientational disorder is introduced within the layer and the molecular orientational distribution function is modeled as a normal distribution, the final intensity becomes the convolution of eq 1 with a Gaussian, and thus the mathematics is analogous to that for diffusion. Equation 1 acts as an initial concentration profile that is smeared accordingly:

$$I(\beta,\Delta) = \pi^{-0.5}\Delta^{-1}\int_{-\phi}^{\phi} I(s)\exp\{-((\beta - s)/\Delta)^2\}\,ds \tag{2}$$

where s is a dummy integration variable. The best fit with the experimental data is found for $\phi = 38°$ and $\Delta = 16°$. A tilt angle of 38° roughly corresponds to the combined effect of vertical spacers and mesogens tilted at 48°. A standard deviation of 16° molecular tilt corresponds to an orientational order parameter ($S = {}^3/_2\langle\cos^2\psi\rangle - {}^1/_2$,

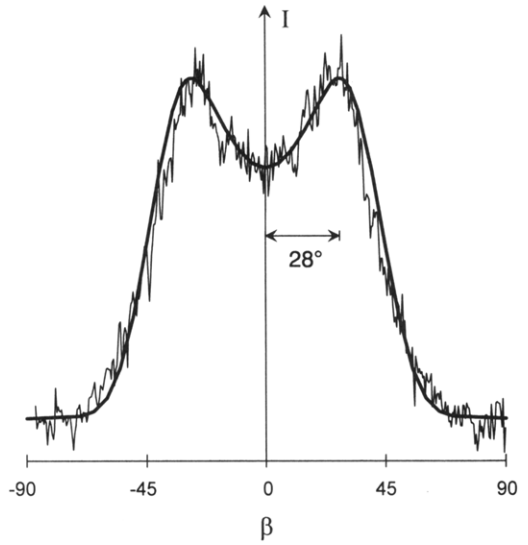

Figure 5. Densitometer scan of the diffuse wide-angle peak in Figure 1a as a function of azimuthal angle fit with the disordered-uniaxial model described in the text.

where ψ is the angle of deviation from the average orientation) within each layer equal to 0.944 (a reasonable value for a C_2 mesophase but too high if the mesophase were microscopically smectic A). The maximum intensity is finally at an azimuthal angle of 28°, in agreement with the data (Figure 5). Thus the fully-extended-chain model (Figure 2) given in a previous publication is likely.[15] More extensive comparison between the molecular model and the diffraction pattern is not practical, since analysis of many conformations would be necessary to simulate the liquid state.

Diffraction also gives additional information regarding disorder. The lack of higher-order meridional reflections (the second order is only very weakly present on the original negative) demonstrates that the density variation along **n** is nearly a sinusoid. In contrast, the peaks that are present are sharp, indicating very long-range order of the layers. The long- and short-range order can effect the diffraction pattern independently. Neither sinusoidal density variation or orientational disorder within layers should significantly influence crystallization; however, as indicated above, the type of distortion that is significant is molecular twisting and accompanying molecular entanglement.

Before discussion of crystallization, we first discuss how molecular twisting is introduced through disclinations present in the smectic C_2 mesophase. Because of the biaxial nature of tilted smectic phases, the orientational state of the material is described by *two* local directors: the layer *normal*, **n**, and the direction of tilt, **C**, *i.e.*, *the projection of the mesogen axis onto the layer plane* (see Figure 2). Disclinations may be present in either of the two director fields. In contrast to smectic C, in which the tilt between layers is in the same direction, the alternating tilts of C_2 cause the **C**-director to be a headless vector like **n**.[22] Thus half-integer disclinations are allowed in the **C**-director. However, because reversal of molecular tilt is accomplished by a translation of half the bilayer repeat, a half-integer **C**-director disclination must be accompanied by a dislocation having a Burger's vector equal to half the bilayer. The combined defect is called a dispiration.[22,24]

We tried to observe **C**-director disclinations using polarizing optical microscopy, but only fine-scale textures were produced. Instead, the disclination density was evaluated from selected-area electron diffraction. The

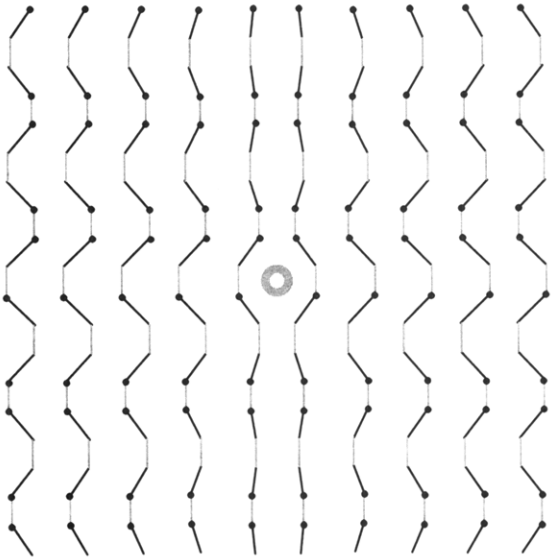

Figure 6. Schematic representation of an integer **C**-director disclination, whose center is marked by a gray circle. As in Figure 3, the dots at mesogen ends indicate the end that is tilting toward the view direction.

result of these disclinations (Figure 6) (whether half-integer or whole integer) is to produce uniaxial symmmetry about **n**, so that the global symmetry is smectic A rather than smectic C or C_2. (A smectic C_2 mesophase might transform to a smectic A through one of at least two possible mechanisms: the chain could straighten its conformation through the introduction of gauche linkages or the transition may be mediated by such disclinations.[25]) In the present case, the disclination density is certainly high ($\sim 10^9/cm^2$) but not unreasonably so for polymeric liquid crystals.[7] A high density of disclinations might be expected since the elastic constants are typically small and the viscosity for polymeric smectics is large.

Crystallization is attained upon thermal annealing (Figure 1b), indicated by the sharp higher-order meridional reflections (i.e., hkl = 003, 004, 005, and 007) and other unassigned peaks off the meridian. The 001 meridional reflection is also sharper. The layer spacing, however, is unchanged. Similar results are found after "solvent treatment" (Figure 1c), indicating that methanol is a suitable plasticizer for crystallization of this LCP. (Annealing without methanol at 40 °C does not result in crystallization.) The new off-meridional reflections play an important role in the simultaneous imaging of both the crystal and the smectic phases.

Having measured the layer spacing from electron diffraction, we could calculate the conditions for imaging the smectic layers. Because the smallest dimension we desire to image (d = 23.4 Å) is an order of magnitude greater than the resolution of the microscope, the optimal focusing can be approximated:

$$\Delta f_{opt} \sim -d^2/(2\lambda) \sim -1.1\ \mu m \qquad (3)$$

where λ is the electronn wavelength, which for 200-kV electrons is 0.025 Å. Therefore, a defocus of ca. −0.96 μm was used to obtain the following images. Furthermore, an objective aperture was used so that high-order, off-meridional reflections would be blocked. In this manner, the smectic layers can be imaged by phase contrast and the crystallites can be imaged by diffraction contrast.

Diffraction contrast is not present in images of quenched samples, but phase contrast clearly reveals the smectic layers (Figure 7). Consistent with prior work on a smectic

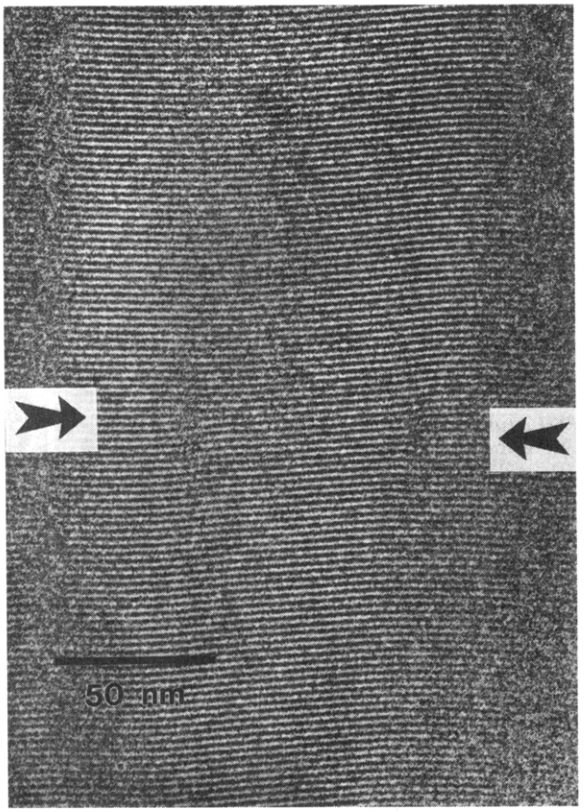

Figure 7. High-resolution electron micrograph of a quenched (smectic C) specimen.

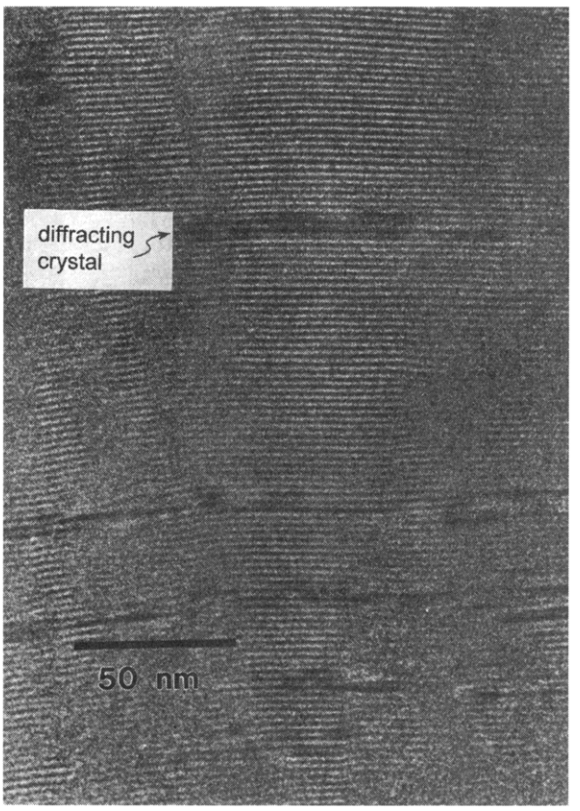

Figure 8. High-resolution electron micrograph of an annealed (semicrystalline) specimen. Diffracting lamellae appear dark.

side-chain LCP,[11] there is high coherence along the director (the layer normal). The layers also extend laterally as well, but the contrast intensity possibly varies as a result of fluctuations in director and/or sample orientation. These fluctuations are sufficiently large in a thin film; therefore, the image is noisy in these regions (at the left and right edges of Figure 7). In-plane director fluctuations are observed as well, evident in the sinuous appearance of the layers. Defects are also present. A pair of oppositely-signed elementary edge dislocations appear midway down in Figure 7, and in other regions of the film compound dislocations (those of the larger Burger's vector) are present as disclination pairs.[26] It is important to note, however, that Burger's vector of these elementary disclinations is one layer, rather than a bilayer. If the mesophase is smectic C_2, then these defects are actually dispirations.[22] A unit dislocation must be accompanied by a half-integer disclination (of twist character since the defect line is perpendicular to the specimen-film plane) in order to have continuity of the smectic phase. Thus the **C**-director disclinations invoked earlier have now been indirectly observed in this material. Other **C**-director disclinations, not associated with dislocations, undoubtedly are present to cause the uniaxial symmetry of electron diffraction, but these lattice images are only able to detect only those defects that distort the smectic layers.

Diffraction contrast is present in images of annealed samples, where diffracting crystals appear darkened, as in Figure 8. The lifetime of the higher-order off-meridional reflections, in the 200-kV electron beam, is approximately half that of the 001; as a result, the diffraction contrast diappears from the image before the layers do. Not all crystallites satisfy the Bragg condition for diffraction; hence, only a few crystallites appear in Figure 8. However, other lamellae can be detected also in bright field, because the 001 reflection is sharpened (Figure 1b,c), thus producing a modulation in the layer contrast (Figure 9). (An

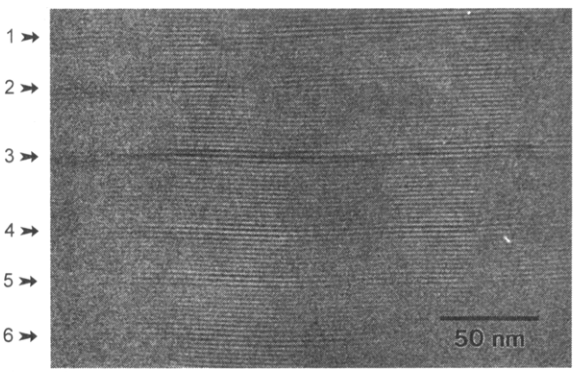

Figure 9. High-resolution electron micrograph of an annealed specimen. Several lamellae are observed here, not by diffraction but by enhanced phase contrast. This micrograph is printed at lower contrast than Figures 7 and 8 in order to highlight the difference between crystal and smectic phases.

alternative interpretation of contrast modulation is disordering of the smectic, but we do not favor this view, since the 001 reflection is sharpened and the contrast within the smectic regions is uniform.) The crystallite no. 3 in Figure 9 is diffracting (darkened), whereas other lamellae above and below are not darkened but only appear as regions of the same size and shape that have greater layer contrast. This mechanism of imaging crystals enables measurement of the lamellar period. Meridional dark field should also be useful. The crystals are only three to four smectic layers thick (approximately 80 Å), and a typical lamellar period (from Figure 9) is approximately 200 Å. Therefore, the crystallinity is quite low, in agreement with NMR results on another semiflexible polymeric smectic[13] and X-ray results on the present polymer.[15]

After synthesis of all of these observations, the reason for the observed lamellar morphology and low crystallinity emerges. Because the layers extend straight through a crystal into the smectic, crystallization probably does not

involve axial shifts, which would disrupt the smectic order, but rather only lateral translations and rotations about the chain axis. Since the overall texture of the film is uniaxial, the orientation of the **a** and **b** crystal axes in the layer plane is different from one lamella to the next. (Uniaxial symmetry also confirms that, although the specimen is thin, the morphology is not influenced by surface effects that would break this symmetry.) Molecular entanglements, as well as C-director disclinations, are excluded from the crystals and thus are concentrated into the intercrystalline smectic phase (Figure 4b). Segregation of entanglements, which are unique to *polymeric* smectics, limits growth, causing the crystallites to be lamellar. Entanglements do not likewise impede lateral growth; hence, lamellae are quite long (in excess of 200 nm). Lesser lateral extent (100–200 nm) was found in solvent-treated samples. Using terminology adapted from extended-chain polymers, the intercrystallite smectic phase is an axial-chain-invariant twist boundary.[21]

An alternative suggestion for thin crystals may be that the growth rate is much faster laterally than axially, as would be implied by a much greater activation energy for nucleation of a step on the lamellar surface compared to that on the edge of a crystal. On the contrary, the surface energy of a step on the lamellar surface is expected to be small, because of the observed continuity of layers across the crystallite boundary. This intuition is confirmed by lamella no. 1 in Figure 9, which is inclined with respect to the layers, yet has the same thickness.

Note that the coherence length along the director in the semicrystalline phase is large (sharp meridional reflections) even though the crystal thickness along this direction is very small (~80 Å). A large coherence length is a consequence of the smectic mesophase, which is not significantly disrupted by crystallization. Morphology of rigid-rod systems is analogous, showing that the crystal thickness is small compared to the coherence length.[27] In the rigid-rod case, the large coherence length results from a molecular property, whereas in our case it results from a coherent phase.

Conclusions

We have investigated the morphology of smectic and semicrystalline phases in a liquid crystalline polymer. The mesophase is smectic C_2, and we have developed a disordered uniaxial analytical model for measuring the molecular tilt angle in any tilted-smectic-phase specimen, in which the *layers* rather than the molecules are aligned. We also successfully employed a high-resolution electron-microscopic technique that allowed simultaneous phase and diffraction contrast. The polymeric nature of these materials causes their crystallization to differ markedly from that of small-molecule smectics. Entanglements exist in the smectic phase, which then segregate during crystallization and limit the growth to thin (~80 Å) lamellae. Such an enrichment of defects outside the crystal seems to cause only a minor disruption of the smectic phase, since the layers are clearly resolved in both phases. We do not known whether the entanglements impose a kinetic limit to the lamellar thickness at high temperatures; another question for further work is determination of the minimum thickness for the axial-chain-invariant boundary between lamellae. Finally, the coherence length in the semicrystalline phase along the chain is large, even though the crystals are very thin (80 Å) in this dimension. The large coherence length results from coherence of the smectic layers.

References and Notes

(1) *Structure and Properties of Polymers*; Thomas, E. L., Ed.; VCH Publishers: Weinheim, Germany, 1993; Vol. 12.
(2) Donald, A. M.; Windle, A. H. *Liquid Crystalline Polymers*; Cambridge University Press: Cambridge, U.K., 1992.
(3) Thomas, E. L.; Wood, B. A. *Faraday Discuss. Chem. Soc.* **1985**, *79*, 229.
(4) Windle, A. H.; Viney, C.; Gulombok, R.; Donald, A. M.; Mitchell, G. R. *Faraday Discuss. Chem. Soc.* **1985**, *79*, 55.
(5) Hudson, S. D.; Thomas, E. L. *Phys. Rev. Lett.* **1989**, *62*, 1993.
(6) Hudson, S. D.; Fleming, J. W.; Gholz, E.; Thomas, E. I. *Macromolecules* **1993**, *26*, 1270.
(7) Hudson, S. D.; Thomas, E. L. *Phys. Res. A* **1991**, *44*, 8128.
(8) Campoy, I.; Marco, C.; Gomez, M. A.; Fatou, J. G. *Macromolecules* **1992**, *25*, 4392.
(9) Kent, S. L.; Geil, P. H. *J. Polym. Sci., Polym. Phys. Ed.* **1992**, *30*, 1489.
(10) Li, M. H.; Brulet, A.; Keller, P.; Strazielle, C.; Cotton, J. P. *Macromolecules* **1993**, *26*, 119.
(11) Durst, H.; Voigt-Martin, I. G. *Makromol. Chem., Rapid Commun.* **1986**, *7*, 785.
(12) Sammon, M. J.; Zasadzinski, J. A. N.; Kuzma, M. R. *Phys. Rev. Lett.* **1986**, *57*, 2834.
(13) Perez, E.; Marugan, M. M.; VanderHart, D. L. *Macromolecules* **1993**, *26*, 5852.
(14) Marco, C.; Lorente, J.; Gomez, M. A.; Fatou, J. G. *Polymer* **1992**, *33*, 3108.
(15) Ellis, G.; Lorente, J.; Marco, C.; Gomez, M. A.; Fatou, J. G. *Spectrochim. Acta, Part A* **1991**, *47*, 1353.
(16) Ellis, G.; Marco, C.; Lorente, J.; Gomez, M. A.; Fatou, J. G., unpublished data.
(17) Galbiati, E.; Zerbi, G.; Benedetti, E.; Chiellini, E. *Polymer* **1991**, *32*, 1555.
(18) Watanabe, J.; Hayashi, M. *Macromolecules* **1989**, *22*, 4083.
(19) Brand, H. R.; Cladis, P. E.; Pleiner, H. *Macromolecules* **1992**, *25*, 7223.
(20) Francescangeli, O.; Albertini, G.; Yang, B.; Angeloni, A. S.; Laus, M.; Chiellini, E.; Galli, G. *Liq. Cryst.* **1993**, *13*, 353.
(21) Martin, D. C.; Thomas, E. L. *Philos. Mag. A.* **1991**, *64*, 903.
(22) Watanabe, J.; Kinoshita, S. *J. Phys. II (Fr.)* **1992**, *2*, 1237.
(23) Watanabe, J.; Komura, H.; Niiori, T. *Liq. Cryst.* **1993**, *13*, 455.
(24) Harris, W. F. *Sci. Am.* **1977**, *237*, 130.
(25) Nelson, D. R. Defect-mediated Phase Transitions. *Phase Transitions and Critical Phenomena*; Domb, C., Lebowitz, J. L., Eds.; Academic Press: London, 1983; Vol. 7, pp 1–99.
(26) Kleman, M. *Points, Lines and Walls*; John Wiley & Sons: Chichester, U.K., 1983.
(27) Panar, M.; Avakian, P.; Blume, R. C.; Gardner, K. H.; Gierke, T. D.; Yang, H. H. *J. Polym. Sci., Polym. Phys. Ed.* **1983**, *21*, 1955.